REPORT DOCUMENTATION PAGE

Form Approved
OMB No. 0704-0188

Public reporting burden for this collection of information is estimated to average 1 hour per response, including the time for reviewing instructions, searching existing data sources, gathering and maintaining the data needed, and completing and reviewing the collection of information. Send comments regarding this burden estimate or any other aspect of this collection of information, including suggestions for reducing this burden, to Washington Headquarters Services, Directorate for Information Operations and Reports, 1215 Jefferson Davis Highway, Suite 1204, Arlington, VA 22202-4302, and to the Office of Management and Budget, Paperwork Reduction Project (0704-0188), Washington, DC 20503.

1. AGENCY USE ONLY *(Leave blank)*	2. REPORT DATE	3. REPORT TYPE AND DATES COVERED
	April 1996	Professional Paper

4. TITLE AND SUBTITLE

IFOG TECHNOLOGY FOR GYROCOMPASS APPLICATIONS

5. FUNDING NUMBERS

PR: NNB1
PE: 0602232N
WU: DN081123

6. AUTHOR(S)

E. Goldner, D. Rozelle, J. De Fato, A. Brockstein, A. Cordova, R. Mlchal, R. Patterson, and J. Steele

7. PERFORMING ORGANIZATION NAME(S) AND ADDRESS(ES)

Naval Command, Control and Ocean Surveillance Center (NCCOSC)
RDT&E Division Detachment
Warminster, PA 18974

8. PERFORMING ORGANIZATION REPORT NUMBER

9. SPONSORING/MONITORING AGENCY NAME(S) AND ADDRESS(ES)

Naval Command, Control and Ocean Surveillance Center (NCCOSC)
RDT&E Division
San Diego, CA 92152–5001

10. SPONSORING/MONITORING AGENCY REPORT NUMBER

11. SUPPLEMENTARY NOTES

12a. DISTRIBUTION/AVAILABILITY STATEMENT

Approved for public release; distribution is unlimited.

12b. DISTRIBUTION CODE

13. ABSTRACT *(Maximum 200 words)*

Interferometric fiber optic gyros (IFOGs) were fabricated and evaluated to demonstrate the feasibility of their use as rotation rate sensors within replacement gyrocompass systems. Bias repeatability of 0.008 deg/hr, input axis misalignment repeatability of 0.68 arcsec, scale factor repeatability of 4.5 ppm, and angle random walk of 0.0034 deg/$\sqrt{\text{hr}}$ were demonstrated. The measured gyro performance was included within system simulations to predict overall system performance for a series of gyrocompass scenarios. The results of the simulations showed that when mechanized with IFOGs similar to those tested, the performance specifications of the AN/WSN-2/2A gyrocompass can be achieved without the need for a vertical axis turntable for periodic self-calibration. IFOGs were shown to be a strong candidate for the rotation rate sensors within upgrades and future Navy gyrocompass systems.

19960524 036

Published in *Proceedings of the 51st Institute of Navigation Annual Meeting*, June 1995.

14. SUBJECT TERMS

Mission Area: Navigation
Interferometric Fiber Optic Gyros (IFOG)
Gyrocompass

15. NUMBER OF PAGES

16. PRICE CODE

17. SECURITY CLASSIFICATION OF REPORT	18. SECURITY CLASSIFICATION OF THIS PAGE	19. SECURITY CLASSIFICATION OF ABSTRACT	20. LIMITATION OF ABSTRACT
UNCLASSIFIED	UNCLASSIFIED	UNCLASSIFIED	SAME AS REPORT

DTIC QUALITY INSPECTED 1

21a. NAME OF RESPONSIBLE INDIVIDUAL	21b. TELEPHONE *(include Area Code)*	21c. OFFICE SYMBOL
J. De Fato	(215) 441–1205	Code 322

IFOG TECHNOLOGY FOR GYROCOMPASS APPLICATIONS

Eric Goldner, David Rozelle, Joseph DeFato*, Allan Brockstein, Amado Cordova,
Ronald Mlchal, Ralph Patterson and James Steele

Litton Guidance and Control Systems
5500 Canoga Ave.
Woodland Hills, CA 91367

*Naval Command, Control and Ocean Surveillance Center
RDT&E Division Detachment
Warminster, PA

BIOGRAPHY

Eric Goldner received his BSME in 1982 and MS in Electrical Engineering in 1986 from Tufts University. He has worked in the Fiber Optic Gyro Engineering Directorate at Litton since 1987. He has been responsible for the development of various aspects of fiber optic gyro technology, including sensor coils, integrated optic chip pigtailing, and gyro optical architecture. He is an author of more than a dozen technical papers and one patent, most in the area of fiber optic gyros.

ABSTRACT

Interferometric fiber optic gyros (IFOGs) were fabricated and evaluated to demonstrate the feasibility of their use as rotation rate sensors within replacement gyrocompass systems. Bias repeatability of 0.008 deg/hr, input axis misalignment repeatability of 0.68 arcsec, scale factor repeatability of 4.5 ppm, and angle random walk of 0.0034 deg/$\sqrt{hr}$ were demonstrated. The measured gyro performance was included within system simulations to predict overall system performance for a series of gyrocompass scenarios. The results of the simulations showed that when mechanized with IFOGs similar to those tested, the performance specifications of the AN/WSN-2/2A gyrocompass can be achieved without the need for a vertical axis turntable for periodic self-calibration. IFOGs were shown to be a strong candidate for the rotation rate sensors within upgrades and future Navy gyrocompass systems.

INTRODUCTION

The spinning mass gyro technology currently in use within Navy shipboard gyrocompass equipment is becoming more costly to support. Reduced procurement costs and higher reliability are critical factors as replacement technologies are considered. The factors governing the ship mission are long endurance, low speed, and slow maneuvers. In support of the Navigation and Aircraft Command, Control Communication and Technology Program sponsored by the Office of Naval Research (ONR) and the Fiber Optic Basic Technology Program sponsored by the Naval Sea Systems Command, the Naval Command, Control and Ocean Surveillance Center (NCCOSC) Research, Development, Test and Evaluation (RDT&E) Division Detachment is assessing the viability of using fiber optic gyro technology for Navy shipboard inertial reference system applications. Fiber optic gyro (FOG) technology has been under consideration for a wide range of military applications for over ten years, with its advantages over older technologies that include lower cost and higher reliability combined with high performance and small size. The successful use of IFOG technology in marine inertial reference systems requires adequate performance levels with respect to gyro bias stability, scale factor, and random walk. The factor that makes ship and submarine navigation unique is the requirement for long-term gyro bias drift and calibration stability in a temperature controlled environment.

Exploratory IFOG development for shipboard gyrocompass system applications has been conducted by NCCOSC RDT&E Division Detachment, Warminster, PA as a subtask of the Navigation System Technology (RC32N10) Project Plan sponsored by ONR. This program has focused on demonstrating the inherent capability of IFOG technology to meet the most stringent performance requirements of the Navy's gyrocompass systems (AN/WSN-2 and 2A), utilized aboard submarines. This effort included NCCOSC test and evaluation of industry first-generation brassboard IFOG models. The NCCOSC evaluation showed the enormous potential this new technology had relative to shipboard inertial measurement and reference applications, and also showed the need for gyro architecture and component improvements to remedy IFOG temperature sensitivity and IFOG light source reliability deficiencies.

With funding support provided by ONR and the Naval Sea System Command, NCCOSC is currently directing the development of a second-generation IFOG design that will be suitable for shipboard gyrocompass applications. This new development incorporates gyro technology advances made to resolve deficiencies associated with the first-generation IFOG designs. In addition to IFOG sensor architecture enhancements, these advances include improved gyro rotation sensing coil fabrication techniques to minimize performance-degrading thermal effects, new light source technology for increased gyro lifetime and reliability, and integrated optic development enabling the manufacture of reduced cost photonics components with improved optical characteristics. As part of this effort, the Guidance & Control Systems Division of Litton Systems was funded to develop an IFOG design intended for use in high accuracy stabilized shipboard gyrocompass equipment. In addition, Litton fabricated and evaluated two second-generation gyrocompass IFOG demonstration units to assess the performance capabilities of the current IFOG technology relative to the requirements of Navy gyrocompass systems under environmental conditions similar to those expected for typical missions. The two demonstration instruments were subsequently delivered to NCCOSC, Warminster, PA, where Navy laboratory test and evaluation of the demonstration units is in progress.

This paper describes the design of the Litton gyrocompass IFOGs, and the features incorporated in the demo units to overcome the deficiencies identified in the first-generation IFOG brassboards identified by NCCOSC. The evaluation of the two demonstration units and the test data obtained during the formal acceptance test procedure (ATP) will be presented. System simulations, based upon expected mission scenarios and the demonstration units' performance values will be discussed, with the results compared to gyrocompass system requirements. Finally, a modular gyrocompass system design approach, based upon an IFOG rotation sensor, will be presented.

SYSTEM/INSTRUMENT REQUIREMENTS

A family of marine gyrocompass systems was studied as potential applications for IFOG-based inertial sensing units. The family included the AN/WSN-2/2A system, the MK-19 Mod 3 gyrocompass, and the MK-23 and MK-27 gyrocompasses. A common set of requirements was developed for these applications. The NCCOSC-supported Litton gyrocompass IFOG program had as its main goals: (a) completion of a commonality study showing how IFOG-based systems could address the requirements of the gyrocompass family studied; and (b) demonstration of the capability of an IFOG to meet the performance requirements flowed down from the systems' requirements. The commonality study concluded that the performance requirements of the AN/WSN-2/2A are the most stringent of the applications considered. Therefore, these performance levels became the goals of the demonstration IFOGs produced under this program. The specific requirements are discussed in this paper relative to the actual performance levels measured and modeled within the system simulations.

GYRO DESIGN

The IFOG is an all-solid-state instrument with no moving parts (unlike its predecessors such as spinning mass gyros and dithered ring laser gyros). The design of the IFOG takes advantage of commercial fiber optic telecommunication technology. This allows for low manufacturing cost and leads to high unit reliability. To further reduce the cost and maximize reliability, the Litton IFOG design approach accommodates a strapdown system mechanization. This also means that the system provides no instrument calibration capability, and the instruments must be designed to be exposed to the full range of operating environments.

The operation of an IFOG is based upon the Sagnac effect [1], the result of which is a relative phase shift between two counterpropagating light waves within a closed path that is proportional to the path's rotation rate relative to a fixed reference. The optical configuration employed in the demo unit design is shown in Figure 1. Litton's improved broadband solid-state light source provides the optical energy for the instrument and represents a significant improvement over the previous generation fiber optic gyro light sources, namely superluminescent diodes (SLDs). SLDs have traditionally suffered from two deficiencies. First, the total optical output power available from a single SLD is typically limited to 0.5 to 1.0 mW over military environments. The instrument angle random walk is thus limited by the shot noise at the photodetector. In addition, SLDs have a wavelength temperature sensitivity of about 300 ppm per degree C, which directly translates into an instrument scale factor temperature sensitivity on the same order. Litton's improved source has shown to be capable of producing far more optical power with greatly enhanced wavelength stability over temperature compared to SLDs.

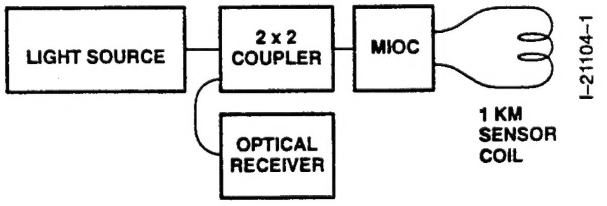

Figure 1. Gyrocompass IFOG Demonstration Unit Optical Configuration Design

The radiation from the source is split by a 2x2 fiber optic coupler (necessary to satisfy reciprocity conditions to minimize bias errors versus temperature [1]). The light continues to the interferometer, comprised of a multi-function integrated optic chip (MIOC) and the optical fiber sensor coil. The integrated optic chip serves three functions. It divides light so that two roughly equal amplitude waves can counterpropagate around the coil. The counterpropagating waves within the interferometer combine coherently at the Y-junction of the integrated optic chip. This chip also contains a pair of phase modulators used for modulating the interferometer for fine resolution of angular rates.

The sensor coil is a 1 km length of polarization maintaining fiber wound in a coil less than 7.0 cm in diameter. Since the previous generation brassboard IFOG models were evaluated by the Navy, Litton has made significant strides in coil design and processing to substantially reduce the sensitivity of the coil to temperature. Older generations of FOG sensor coils suffered from high sensitivity to the time rate of change of temperature within the coil. This effect was described by Shupe in 1980 [2]. This effect is one in which heat flow through the coil causes small changes in the length or refractive index of a fiber segment that affects the optical path traversed by the two counterpropagating waves slightly differently due to the finite speed of light, causing a nonreciprocal phase shift which is indistinguishable from real rotation rate [3]. In 1983, Frigo proposed a method for minimizing this effect, in which the fiber is wound in a quadrupolar fashion [4]. This method has been developed at Litton and utilized for factory production of tactical-grade IFOGS. A proprietary coil design and winding process has allowed Litton to reduce the bias sensitivity due to time-varying thermal gradients within the coil by two orders of magnitude and improve the bias modelability of the gyros over dynamic thermal environments.

After the waves recombine at the Y-junction, the resulting light (containing the rotation rate information) continues back to the 2x2 coupler, and from there to the optical receiver, which is an integrated photodiode/high gain transimpedance amplifier (optical receiver).

Litton's IFOGs are operated using a closed loop modulation/demodulation technique. This ensures high sensitivity to rotation rate, high scale factor linearity, and minimal bias errors that result from changes in source output power or gyro optical loss. As shown in Figure 2, the optical receiver output is amplified and converted to a digital signal. The digital signal processor uses the digitized

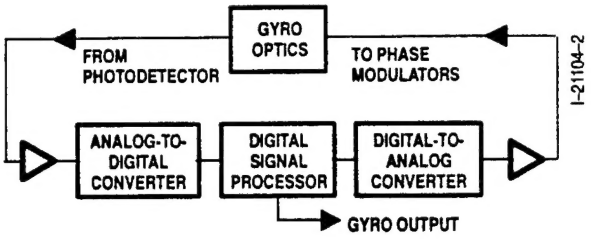

Figure 2. Closed-Loop Modulation/ Demodulation Block Diagram

receiver signal to create an opposing signal that is applied to the phase modulators (via an analog-to-digital converter). That signal seeks to null the receiver output. The resulting phase modulator drive signal is a measure of the sensed rotation rate, and the servo loop attempts to operate at a null point.

This type of optical architecture allows for a system that is easily producible and lends itself to being manufactured using automated processes, thus allowing for low cost production. An added feature of this type of architecture is its ability to be packaged in many different form factors. This allows the IFOG instrument to be used for many different applications without the expense of having to be completely redesigned. The flexibility of this design has allowed for significant reductions in the size and weight of systems utilizing the IFOG without sacrificing the demonstrated high performance of engineering demonstration models.

In addition to the modulation/demodulation electronics, the demonstration units included electronics to stabilize the source output wavelength over time. This is necessary to be able to meet long-term scale factor repeatability requirements.

The packaging of the IFOG for this program is shown in Figure 3. This configuration consists of three elements: the compact coil subassembly, the electronics module, and an umbilical joining the two assemblies. The coil subassembly contains the sensing coil, the MIOC, the MUX coupler, the temperature sensors, and a high magnetic permeability shield. The electronics module contains power supplies, signal processing electronics, optical source and source driver electronics, MIOC drive electronics, and the receiver with its associated preamplifier electronics. The umbilical which joins the two assemblies contains temperature sensor wires, MIOC drive cable, two optical fibers, and a strength member to mechanically stiffen the assembly for handling. For typical IFOG applications, system electronics and the coil subassembly would reside in a common chassis, thus eliminating the need for an umbilical connection. For this demonstration program, however, the

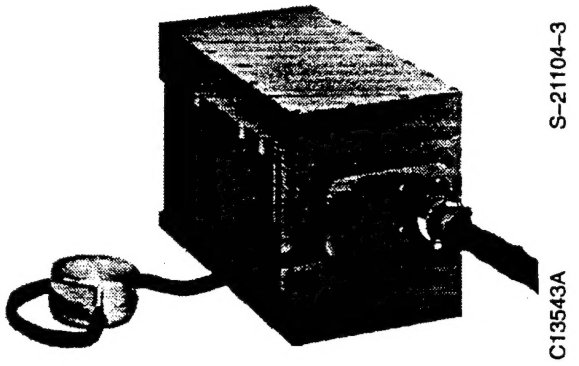

Figure 3. Packaging of the Gyrocompass IFOG Demopnstration Units. *The coil subassembly is shown at left, connected to the elecronics module with an umbilical.*

umbilical provided the capability of assessing the performance of the optics under input axis alignment testing.

GYRO EVALUATION

To assess the suitability of the IFOG technology within the context of a shipboard gyrocompass system, a series of performance evaluation tests was performed at Litton's Woodland Hills, CA facility on the two demonstration units. The testing consisted of random walk, bias, scale factor and input axis alignment characterization as part of the ATP. Thermal behavior, stability and day-to-day repeatability were measured for the parameters as part of the evaluation.

TEST CONFIGURATION

The performance testing was accomplished using a standard testing suite. The gyros were mounted on a single-axis rate table within an environmental chamber. The rate table was mounted on a seismic isolation pier to ensure a stable reference platform. The thermal chamber allowed control of the instrument temperature. During the 30-day bias drift, a second stage thermal chamber (actively controlled via peltier heater/cooler modules) surrounded each coil subassembly, providing further thermal isolation of the gyros from external temperature variations.

The demodulated gyro outputs were in the form of pulse trains (1.25 arcsec per pulse). Sums of pulses were acquired periodically using a commercial counter/timer and recorded on a computer hard disk for post-processing. A series of temperature sensor resistances was measured with a commercially available data acquisition unit to observe thermal sensitivities of individual gyro components.

LITTON TEST RESULTS

Three aspects of the gyro bias were investigated: day-to-day repeatability, constant temperature stability, and bias thermal modelability. Of primary importance for gyrocompass applications is the repeatability. This quantity was measured by observing the bias of each gyro periodically over a two-hour period at 25°C. Between each of these bias drift runs, the gyros were subjected to dynamic environments. After observation of the bias at five points in time spaced over a two-month period, the standard deviations of the sets of bias measurements were determined. The set of the biases are shown in Figure 4. The standard deviations, representing the bias repeatabilities of the two instruments, were 0.008 and 0.033 deg/hr (one sigma) for Demonstration Units No. 1 and No. 2, respectively.

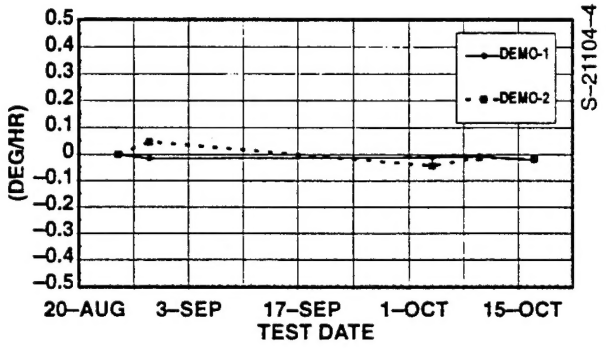

Figure 4. Bias Repeatability of Demonstration Units Nos. 1 and 2

Constant temperature bias stability was measured during a 34-day drift test, with the instruments' sensitive axes facing true north, using a polar mount, thus minimizing the influence of input axis alignment errors. The bias of each gyro was observed continuously while the gyro's temperature was maintained at 25°C, and the data were post-processed using the TRW-developed Autofit algorithm [5]. From this test, the angle random walk was shown to be 0.0038 and 0.0033 deg/$\sqrt{hr}$ for Demonstration Units No. 1 and No. 2, the rate random walk was 0.00019 and 0.00029 deg/hr/$\sqrt{hr}$, and the correlated bias noise was 0.007 deg/hr with a 6-hour correlation time for Demonstration Unit No. 1 and unmeasurable for Demonstration Unit No. 2. The significance of the low rate random walk and correlated noise is that it shows that a gyrocompass system using an IFOG of this design would not need to utilize a vertical axis rate table for periodic system calibration through gyro rotation. From the 33-day bias drift, the bias trend was also calculated and determined to be $1.3 * 10^{-5}$ and $3 * 10^{-5}$ deg/hr/hr for Demonstration Units No. 1 and No. 2. Figure 5 shows the bias drift data and the Allan variance results obtained from this experiment, performed with Demonstration Unit No. 1.

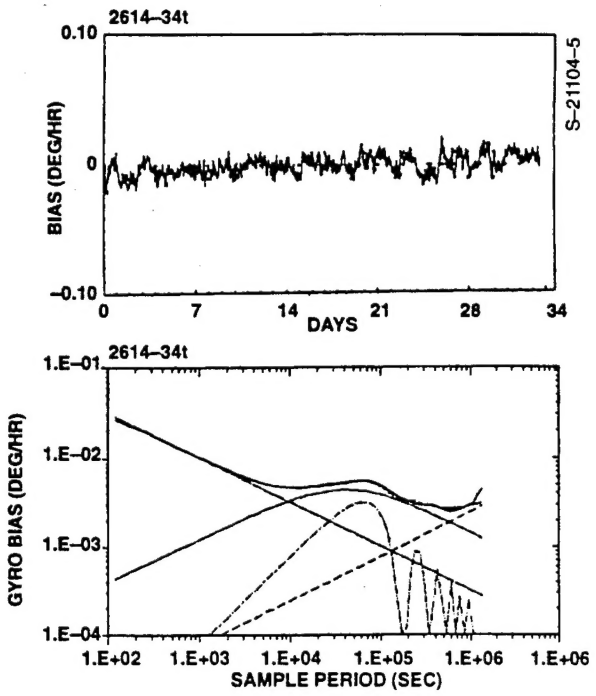

Figure 5. 34-Day Constant Temperature Bias Drift of Demonstration Unit No. 1. *The upper plot shows the bias versus time. The bottom plot shows the Allan variance results. The Allan variance shows correlated noise to be 0.007 deg/hr.*

The gyro bias modelability is a parameter critical to most inertial measurement systems. It predicts the dynamic performance of such an instrument within a system and provides a measurement of the correlated noise of the gyro expected under dynamic thermal conditions. Both gyros demonstrated 0.007 deg/hr residual bias after application of a thermal model and a 30-minute triangular filter (to separate angle random walk effects). An example of this is shown in Figure 6. The plot shows the residual after fitting to a thermal model based upon the 4 to 50°C thermal profile that was applied to the gyro. This profile is shown in Figure 7.

The bias model stability is a measure of the residual bias error of a gyro subjected to dynamic environments, after compensation using model coefficients obtained during an earlier bias calibration test. To characterize the gyro bias residuals after thermal modeling, a dynamic thermal test profile was developed, simulating the worst-case thermal dynamics for a marine gyrocompass. To this end, thermal ramps between 4 and 50°C at rates of 0.5 and 2.2°C/hr were used. To establish the thermal model, a calibration thermal profile was developed that contained these plus two higher ramp rates (15 and 30°C/hr) and an extended temperature range which minimizes the uncertainty of the modeling coefficients at the temperature extremes. Two months

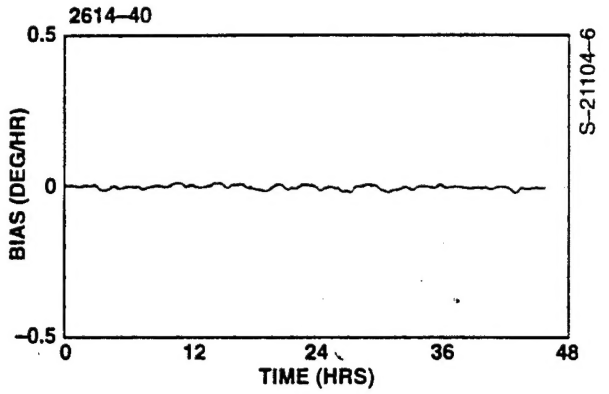

Figure 6. Bias Modelability of Demonstration Unit No. 2. *One-sigma residual was 0.0069 deg/hr after application of a thermal model and a 30-minute filter.*

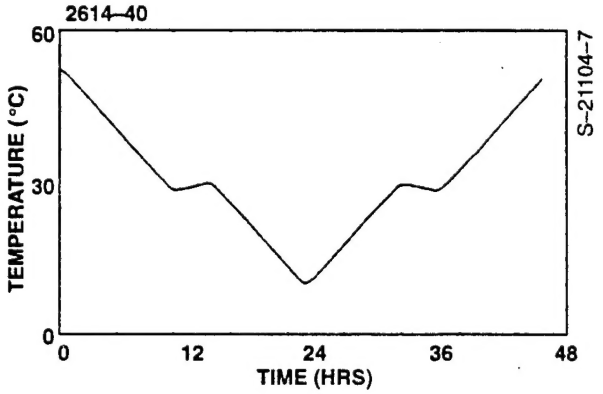

Figure 7. Thermal Profile Applied to the Demonstration Units During Bias Modelability Testing

later, the gyros were subjected to the test profile and the modeled bias residuals were 0.016 and 0.07°/hr (one sigma) after application of a 30-minute triangular filter. As an example, Figure 8 shows the residual bias of Demonstration Unit No. 1 after modeling (with coefficients derived two months earlier).

During ATP, the scale factor of the demonstration units was evaluated from four different standpoints, the linearity, asymmetry, repeatability, and model stability. Linearity of the gyros scale factor was measured at constant temperature. The gyros were rotated from +100 deg/sec to -100 deg/sec in 1 deg/sec intervals. After compensation of the data for thermal variations of the LN_2 chamber temperature control, the scale factor linearities of the two instruments were 1.09 and 2.06 parts per million (ppm). The asymmetry of the scale factors with respect to zero rotation rate was 0.28 and 0.62 ppm for Demonstration Units No. 1 and No. 2, respectively.

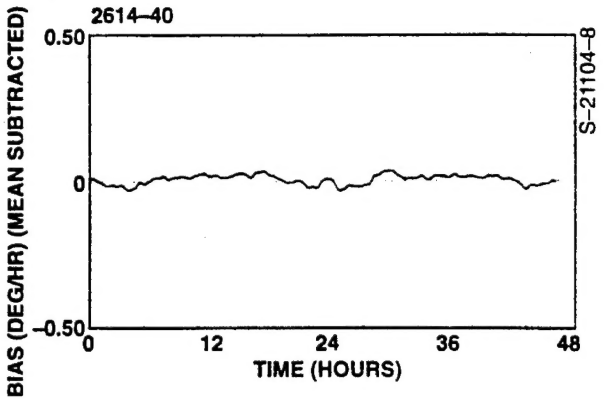

Figure 8. Bias Model Stability. *Residual bias during a thermal profile after application of a thermal model derived two months earlier.*

Measurement of the gyro scale factor repeatability was performed at constant temperature. The gyro was rotated at +/-30 deg/sec, and the scale factor measured for one hour. These measurements were made periodically over a two-week period, and the gyros were subjected to dynamic environments between measurements. The results of this testing were repeatabilities of the gyro scale factor of 9.8 ppm and 4.5 ppm for units 1 and 2, as shown in Figure 9.

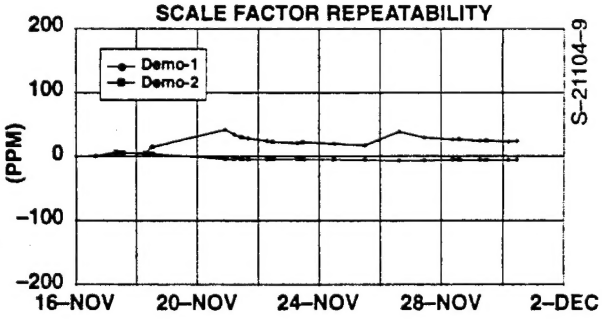

Figure 9. Scale Factor Repeatability. *Points represent average scale factor at 25°C. Means were removed. Standard deviations for each demonstration unit were 9.8 ppm and 4.5 ppm, respectively.*

To assess the dynamic behavior of the gyro scale factor, the modelability of the scale factor was measured over temperature. During these tests, the residual scale factor error of each gyro was determined after applying a thermal model. With gyro temperatures varying between 5 and 50°C at ramp rates of ±5°C/hour, the residual scale factor error after application of calibration coefficients was 11.0 and 3.9 ppm for Demonstration Units No. 1 and No. 2.

The input axis (IA) alignment errors observed included repeatability and model stability. The IA alignment repeatability was measured for each gyro at 25°C periodically over a two-month period. The results of these measurements are shown in Figure 10, in which the one-sigma repeatabilities are 0.68 and 1.2 arcsec for Demonstration Units No. 1 and No. 2, respectively. Analogous to the bias and scale factor model stability measurements, the IA alignment model stability was assessed. The gyros were exposed to a temperature range from 5 to 50°C at ±5°C/hr. During the thermal cycling, the IA alignment error was measured. The resulting data were compensated using a model whose coefficients were established during a calibration procedure. The resulting residuals were 0.073 and 0.28 arcsec (one sigma) for Demonstration Units No. 1 and No. 2.

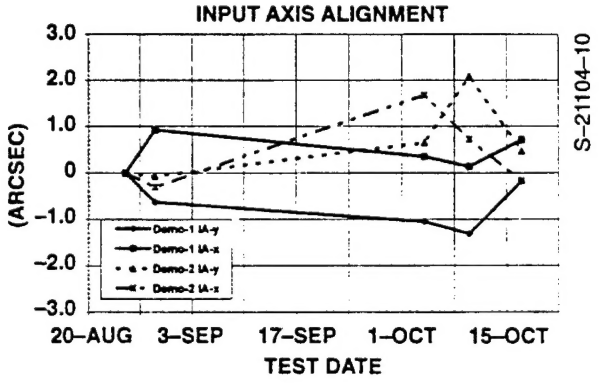

Figure 10. IA Axis Alignment. *Shown are the variations of the IA alignment along two arbitrary axes (x and y) of each gyro. The one-sigma composite errors were 0.68 and 1.2 arcsec for Demonstration Units Nos. 1 and 2, respectively.*

NAVY TESTING OF DEMONSTRATION UNITS

After Litton's evaluation of the two demonstration IFOGs, the instruments were shipped to the NCCOSC RDT&E Division Detachment for subsequent validation testing at NCCOSC's Warminster Inertial Navigation Facility (INFAC). To date, both gyros have been integrated with the Navy's test equipment, and preliminary testing has been completed. Angle random walk was measured for both instruments and is in close agreement with the measurements made at Litton's California facility. The scale factor linearity, asymmetry, repeatability, and temperature sensitivity of both gyros were measured at INFAC, and they agree well with the data obtained by Litton. A comparison between the Litton test data and data obtained by the Navy is shown in Table 1.

Table 1. Comparison of Litton and Navy Test Results of Demonstration Units

Performance Parameter	Units	Goal	Litton Test Results		Navy Test Results	
			Demo No. 1	Demo No. 2	Demo No. 1	Demo No. 2
Angle Random Walk	deg/$\sqrt{hr}$	0.004	0.0028	0.0033	0.0048	0.0038
Scale Factor						
Linearity	ppm	10.0	1.09	2.06	1.5	1.7
Asymmetry	ppm	1.0	0.28	0.62	0.84	0.37
Repeatability	ppm	20.0	9.8	4.5	4.4	12.0
Temperature Sensitivity	ppm/°F	17.0	5.8	12.2	5.36	7.36

SYSTEM SIMULATIONS

The predicted performance of the IFOG shipboard gyrocompass system presented in this section is based on actual data obtained from test data of the two demonstration units collected during ATP. In addition, the simulation includes all known and important error sources associated with the accelerometers and other real-world effects.

Simulation capability at Litton is provided by the RAIDES (RF-Astro-Inertial-Doppler Error Simulation) program. It is used to obtain estimated system performance for specific missions, establish navigation sensor error specifications, develop integrated system mechanizations for Kalman as well as conventional gain designs, validate error model development, and provide test case data for system real-time software checkout. RAIDES is a well validated program that has been used and improved for more than 25 years. Past experience shows that results of the simulation program compare well with actual system test data, thereby providing confidence in its validity as a powerful design tool.

IFOG error parameters found from the ATP were used to generate the gyro portion of the error budget shown in Table 2. In addition, the models associated with the accelerometers, inertial navigation system initial conditions, gravity, EM-log, and water motion are included. The EM-log is a sensor that obtains ship's speed with respect to the water and performs as a speed reference over the long at-sea mission.

Two simulation runs are shown in order to verify that the error budget can meet the AN/WSN-2/2A gyrocompassing requirements [4 arcmin secant (latitude)]. The first scenario consists of a simple 30-hour straight course starting at 65 degrees latitude and heading of 45 degrees. The ship speed, beginning at 30 knots, changes 5 knots every 2 hours and varies between 15 and 40 knots over the mission. The second scenario has the same starting point and speed profile as the first scenario except that a 90-degree clockwise turn at 10 hours and a 90-degree counterclockwise turn at 20 hours are added (with this pattern repeated every 10 hours for a total of 90 hours). The simulation assumes that the ship speed is damped by the EM-log, and a 19-state Kalman filter is mechanized, which performs updating every 5 minutes using the EM-log as an external reference. The 19 error states of the filter include: position (2), velocity (2), attitude (3), gyro bias (3), accelerometer bias (2), gravity deflection (2), EM-log (3), and water motion (2).

Table 2 shows the major error sources for azimuth error at 30 hours for both scenarios. The principal error sources for both cases are gyro correlated noise and gyro bias, respectively. The two 90-degree turns in the second scenario provide variations to the platform orientation, which aid the Kalman filter to resolve the ambiguity between azimuth error and east gyro drift. Therefore the azimuth error is significantly reduced for this scenario.

Figure 11 shows a plot of azimuth error for the first scenario as well as the azimuth requirement as a function of latitude in order to show compliance. Plots for the second scenario are shown in Figures 12 and 13. Figure 12 shows the north tilt (component of attitude error about a local level axis). After the first turn at 10 hours, the tilt is reduced considerably as the heading changes in this scenario help resolve the ambiguity between tilts and accelerometer biases. The before-turn value is the same as obtained for the first scenario, which is still considerably below requirements. Figure 13 shows that the azimuth error is also improved compared to Figure 11, and is well below the requirement. The magnitudes of the attitude errors are well maintained throughout the entire 90-hour mission with no reason to expect that the attitude errors will grow over a longer mission.

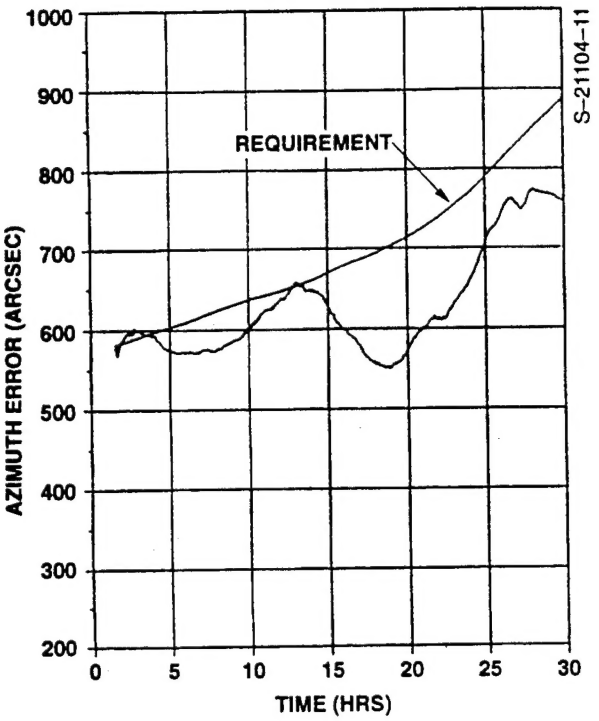

Figure 11. Azimuth Error and Requirements for Scenario 1 (no turns)

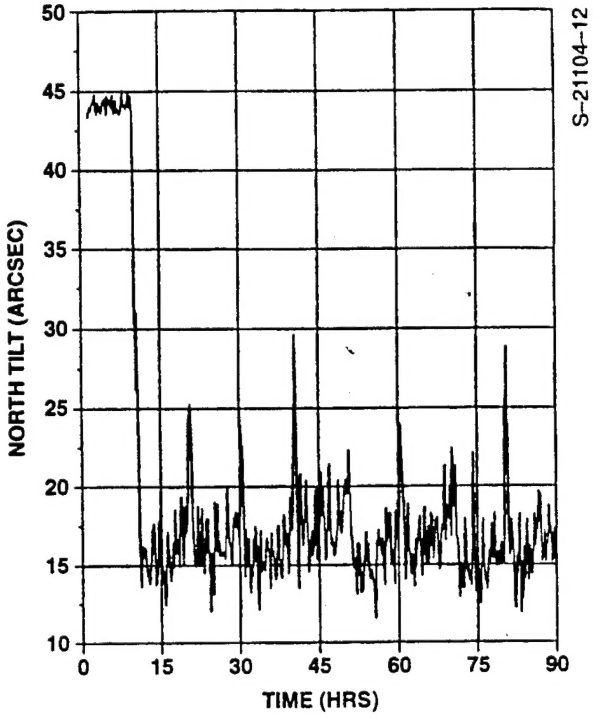

Figure 12. North Tilt for Scenario 2 (turns every 10 hours)

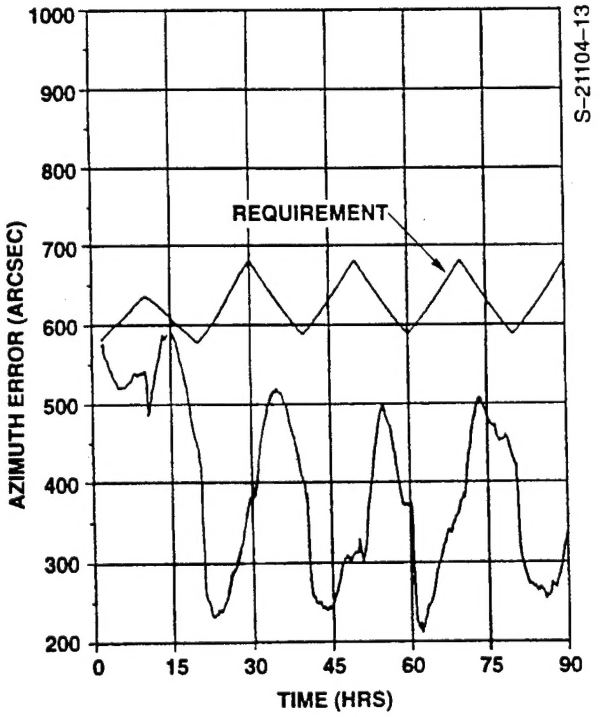

Figure 13. Azimuth Error and Requirements for Scenario 2 (turns every 10 hours)

Table 2. Gyrocompass Error Budget and Sources of Azimuth Error at 30 Hours

Error Parameter	Budget	Azimuth Error (arcsec)	
		Scenario 1 (without turns)	Scenario 2 (with turns
GYRO			
Bias (deg/hr)	0.01	461	230
Scale Factor (ppm)	50	10	8
Scale Factor Asymmetry (ppm)	1	0	0
Misalignment (arcsec)	2	1	2
White Noise (deg/$\sqrt{hr}$)	0.004	166	101
6-hour Correlated Noise (deg/hr)	0.007	515	241
Rate Random Walk (deg/hr/$\sqrt{hr}$)	0.0003	95	55
Trend (deg/hr/hr)	0.00003	40	24
ACCELEROMETER			
Bias (μg)	200	149	17
Scale Factor (ppm)	100	0	0
Scale Factor Asymmetry (ppm)	10	0	0
Misalignment (arcsec)	10	36	4
White Noise (μg/$\sqrt{Hz}$)	50	2	2
30-minute Correlated Noise (μg)	10	13	15
INITIAL NAVIGATION ERROR			
Tilt (deg)	0.5	2	0
Azimuth (deg)	2	3	2
GRAVITY		18	18
Deflection (μg)	25	–	–
Disturbance (μg)	35	–	–
EM-LOG			
Bias (kt)	1	121	27
Scale Factor (%)	2	97	63
Boresight (deg)	1	93	119
White Noise (kt/$\sqrt{Hz}$)	0.048	3	2
1-Hour Correlated Noise (ft)	0.2	15	44
WATER MOTION (kt)	1	71	89
Total (RSS)		760	393

GYROCOMPASS SYSTEM DESIGN

As part of the gyrocompass IFOG development effort supported by the Navy, Litton proposed a system design approach that would satisfy the requirements of the entire family of shipboard applications studied. The design approach is an extremely modular one, incorporating a standard ISU based upon an IFOG as the rotation sensing instrument. Gyrocompass systems containing IFOG rotation sensors can be made at a very low cost. At the heart of the system is a standard IFOG-based strapdown inertial sensing unit (ISU). The ISU is common to other high accuracy systems intended for other (non-shipboard) applications. It contains three axes of gyro optics and accelerometers mounted to a common sensor block. In addition, an ISU contains a processor/controller card for the gyros, a source card containing the optical source and its control electronics, an accelerometer controller, and a power supply. These elements are housed in a common, environmentally rugged enclosure that is expected to occupy about 100 cubic inches. To this core assembly, additional electronics cards providing further features (I/O, GPS, ship's power conversion, external signal conversion, etc.) can be added with appropriate interfaces, software and electronics packaging.

Maintainability of a gyrocompass system is an aspect critical to its cost effectiveness. A standard IFOG-based gyrocompass would include self-test capability for failure diagnosis. Unit level replacement would be made in the field, with card level replacement or submodule repair made at the factory.

Reliability predictions have been developed for an IFOG, the rotation sensing element of a gyrocompass system. Based upon operation within a Navy Sheltered (NS) environment, the expected reliability of the constituent elements and the entire instrument are shown in Table 3. The expected mean time before failure (MTBF) is greater than 150,000 hours for each gyro of a three-axis IFOG triad, including electronics cards.

Table 3. Expected Reliability of a Gyrcompass IFOG and its Constituent Elements

Triad Assembly Part	Failure Rate (per Million Hours)
Source	1.6478
Coupler	0.0082
Photodetector	1.1275
Coil	0.5644
MIOC	0.1784
Splices	0.0264
Interconnect Assembly	0.0181
Source Card	7.1313
Preamplifier Card	4.3983
Processor Card	3.7837
Total Failure Rate	18.8841
Triad MTBF	52,955 hrs
Single Axis MTBF	158,865 hrs

CONCLUSIONS

As a result of the advancements made in light source design, sensor coil development and integrated optic processing, acceptance testing of Litton's current generation of IFOGs demonstrated performance levels needed to support the next generation of shipboard gyrocompass systems. The demonstration units showed performance of 0.008 deg/hr bias repeatability, less than 50 ppm total scale factor error (including better than 10 ppm repeatability and 12 ppm residual error over dynamic thermal environment), less than 1 arcsec input axis alignment error, and 0.004 deg/$\sqrt{\text{hr}}$ angle random walk. Through detailed system simulations, these errors were shown to be consistent with the AN/WSN-2/2A gyrocompass performance requirements. Based upon a single IFOG instrument design, reliable, maintainable and modular gyrocompass systems can be developed that can service a broad range of shipboard applications, with minor modifications needed for specific system configurations. The low rate random walk (0.0003 deg/$\sqrt{\text{hr}}$) allows a system mechanization that does not require a vertical axis turntable for periodic cancellation of bias errors. The solid-state nature and maturity of the technology (especially with the synergy between fiber optic gyros and telecommunications) afford low life cycle cost for such systems from the combination of low acquisition cost and high reliability of the gyros.

REFERENCES

[1] S. Ezekiel and H.J. Arditty, Eds., Fiber Optic Rotation Sensors, Springer Series in Optical Sciences, 32, Springer-Verlag, NY (1982).

[2] D.M. Shupe, "Thermally induced nonreciprocity in the fiber-optic interferometer," Appl. Opt., 19, 654 (1980).

[3] G. Chin, A. Cordova and E. Goldner, "Extended Environmental Performance of Attitude and Heading Reference Grade Fiber Optic Rotation Sensors," Proc. SPIE, 1367, 107 (1990).

[4] N.J. Frigo, "Compensation of linear sources of nonreciprocity in Sagnac interferometers," Proc. SPIE, 412, 268 (1983).

[5] D. Sargent and B.O. Wyman, "Extraction of stability statistics from integrated rate data," AIAA Guidance and Control Conference, Danvers, MA (1980).